

# Structure of a SLC26 Anion Transporter STAS Domain in Complex with Acyl Carrier Protein: Implications for *E. coli* YchM in Fatty Acid Metabolism

Mohan Babu,<sup>1</sup> Jack F. Greenblatt,<sup>1,2</sup> Andrew Emili,<sup>1,2</sup> Natalie C.J. Strynadka,<sup>3</sup> Reinhart A.F. Reithmeier,<sup>4</sup> and Trevor F. Moraes<sup>3,4,\*</sup>

<sup>1</sup>Banting and Best Department of Medical Research, Terrence Donnelly Centre for Cellular and Biomolecular Research, University of Toronto, 160 College Street, Toronto, ON M5S 3E1, Canada

<sup>2</sup>Department of Molecular Genetics, University of Toronto, 1 King's College Circle, Toronto, ON M5S 1A8, Canada

<sup>3</sup>Department of Biochemistry and Molecular Biology and the Centre for Blood Research, University of British Columbia, Life Sciences Centre, 2350 Health Sciences Mall, Vancouver, BC V6T 1Z3, Canada

<sup>4</sup>Department of Biochemistry, University of Toronto, 1 King's College Circle, Toronto, ON M5S 1A8, Canada

\*Correspondence: [trevor.moraes@utoronto.ca](mailto:trevor.moraes@utoronto.ca)

DOI 10.1016/j.str.2010.08.015

## SUMMARY

*Escherichia coli* YchM is a member of the SLC26 (SulP) family of anion transporters with an N-terminal membrane domain and a C-terminal cytoplasmic STAS domain. Mutations in human members of the SLC26 family, including their STAS domain, are linked to a number of inherited diseases. Herein, we describe the high-resolution crystal structure of the STAS domain from *E. coli* YchM isolated in complex with acyl-carrier protein (ACP), an essential component of the fatty acid biosynthesis (FAB) pathway. A genome-wide genetic interaction screen showed that a *ychM* null mutation is synthetically lethal with mutant alleles of genes (*fabBDHGA1*) involved in FAB. Endogenous YchM also copurified with proteins involved in fatty acid metabolism. Furthermore, a deletion strain lacking *ychM* showed altered cellular bicarbonate incorporation in the presence of NaCl and impaired growth at alkaline pH. Thus, identification of the STAS-ACP complex suggests that YchM sequesters ACP to the bacterial membrane linking bicarbonate transport with fatty acid metabolism.

## INTRODUCTION

The human solute carrier SLC26 (solute carrier 26) family of anion transporters consists of 11 members that are expressed in polarized cells in organs such as the kidney, pancreas, intestine, and liver, where they mediate sulfate, chloride, and bicarbonate transport across the plasma membrane (Mount and Romero, 2004). SLC26 transporters consist of an N-terminal membrane domain and a C-terminal terminal STAS domain, an acronym for "Sulfate Transporter Antagonist of anti-Sigma factor" (Aravind and Koonin, 2000). Mutations in the membrane domain as well as the STAS domain of SLC26 transporters cause an array of human diseases, including congenital chloride diarrhea (CLD) in the case of SLC26A3, deafness (Pendred's syndrome)

in the case of SLC26A4, and diastrophic dysplasia in the case of SLC26A2, suggesting that the STAS domain contributes to biosynthetic, functional, or regulatory aspects of these anion transporters (Everett et al., 1997; Everett and Green, 1999; Shibagaki and Grossman, 2004). Additionally, the STAS domains of human SLC26 A3, A4, A5, A6, and A9 have been shown to interact with the R-domain of the cystic fibrosis transmembrane conductance regulator (CFTR) (Chang et al., 2009; Homma et al., 2010; Ko et al., 2002; Shcheynikov et al., 2008), signifying that STAS domains can mediate protein interactions.

The ability of some mammalian members of the SLC26 family (SLC26A3, A4, A6, A7, and A9) to mediate bicarbonate transport has been well documented (Chang et al., 2009; Jiang et al., 2002; Kim et al., 2005; Melvin et al., 1999; Shcheynikov et al., 2008; Xie et al., 2002). Some bacterial members of the SLC26/SulP family contain a C-terminal carbonic anhydrase domain (*Mycobacterium tuberculosis*) or are expressed with carbonic anhydrase in the same operon (*Pseudomonas aeruginosa*), suggesting that these proteins may also transport bicarbonate (Felce and Saier, 2004). *E. coli* overexpressing the SulP protein Rv1739c from *Mycobacterium tuberculosis* however exhibits enhanced sulfate uptake (Zolotarev et al., 2008). BicA from the marine cyanobacterium *Synechococcus* spans the membrane 12 times and contains a C-terminal STAS domain (Shelden et al., 2010). It has been suggested that BicA is a sodium-dependent bicarbonate transporter, although this transport activity has not been demonstrated directly (Price et al., 2004). In *Escherichia coli*, YchM is the only member of the SulP family and is annotated in EcoCyc ([www.ecocyc.org](http://www.ecocyc.org)) as a putative sulfate transporter but its transport properties have not been characterized. YchM is not encoded within an operon and is a nonessential gene when screened for growth at neutral pH (Baba et al., 2006). It consists of 550 amino acids and has two principal structural domains, an N-terminal transmembrane domain predicted to span the bacterial inner membrane 10–12 times (residues 1–435), and a C-terminal cytoplasmic domain (residues 436–550) encompassing the STAS domain of unknown function (Figure 1A). (There are two potential Met encoding start codons for *E. coli* YchM. The amino acid numbering in this manuscript uses the second Met as the amino acid 1, generating a 550 amino acid protein in accordance with NCBI reference sequence: YP\_001458029.1). The

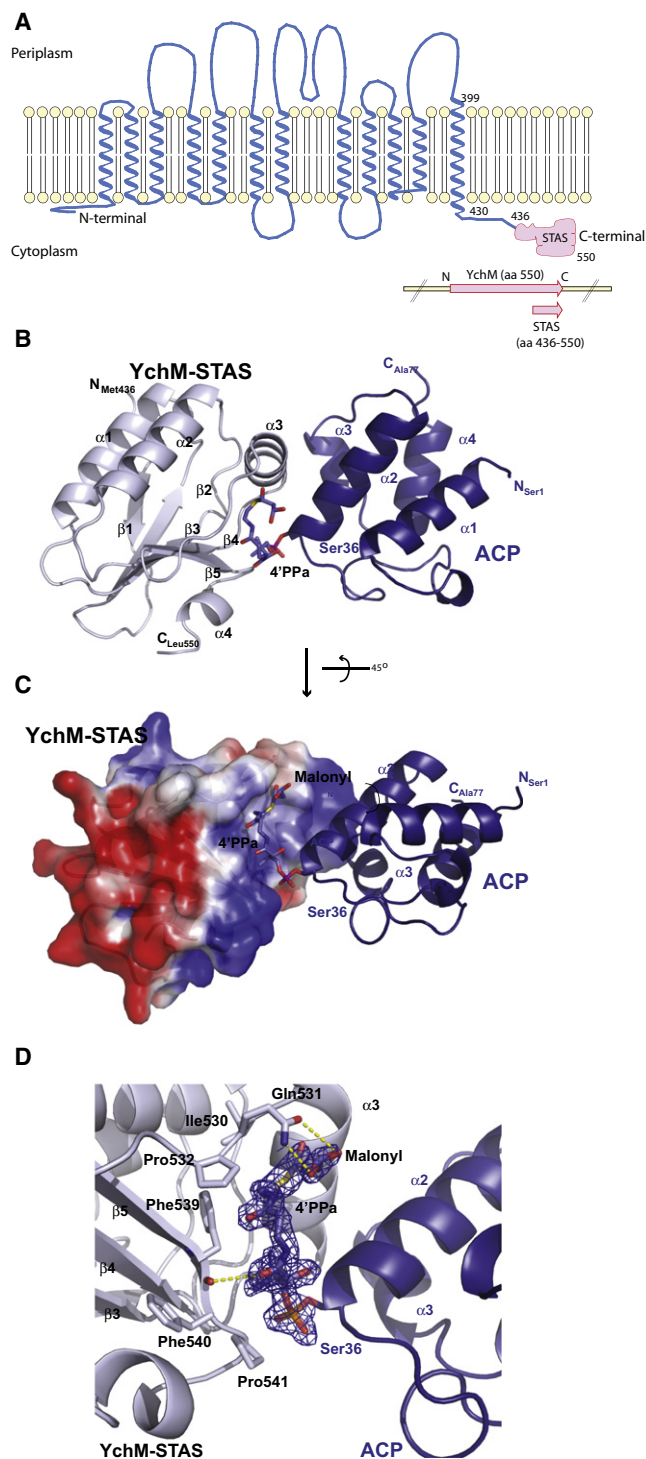


**Figure 1. Structural Analysis of the Cytoplasmic STAS Domain of YchM**

(A) Graphical representation of the YchM protein with an N-terminal membrane domain consisting of 12 predicted transmembrane helices, based on the topology of BicA (Shelden et al., 2010), spanning the bacterial inner membrane and a C-terminal STAS domain (residues 436–550) extending into the cytosol. The YchM transmembrane helices are modeled using TransMembrane Protein Re-Representation in 2 Dimensions (TMRPres2D) software tool. Shown on the

STAS domain of YchM shares 25% sequence identity with the *Bacillus antisigma* factor antagonist SpoIIAA (Dorwart et al., 2008b) that triggers sporulation by interacting with the antisigma factor SpoIIAB (Aravind and Koonin, 2000).

To gain insight into the molecular role of YchM as a transporter of the SulP family in *E. coli* and its STAS domain in particular, we determined the structure of the STAS domain using X-ray crystallography. Strikingly, the STAS domain expressed in *E. coli* copurified in a 1:1 complex with acyl carrier protein (ACP) and its high-resolution crystal structure revealed a specific interaction between ACP and the STAS domain of YchM. In *E. coli*, ACP is an abundant 77 residue protein (0.25% of total soluble protein,  $\sim 5 \times 10^4$  molecules/cell) that runs anomalously slowly upon SDS-PAGE gels (Byers and Gong, 2007a; Niki et al., 1992). ACP contains a 4'-phosphopantetheine group (4'-PPa) covalently attached to Ser36 that acts as an activated thiol ester carrier of acyl intermediates during fatty acid biosynthesis (FAB) and other acylation reactions (Byers and Gong, 2007b) such as the biosynthesis of lipid A (Anderson and Raetz, 1987) and phospholipids (Rock and Jackowski, 1982). ACP is an essential component of the FAB pathway and the C-terminally affinity-tagged ACP protein, encoded by *acpP*, has been shown to interact with a variety of proteins (e.g., MukB, SpoT, SecA, LpxD), including FabB, FabFGH, FabZ, and AcpS involved in FAB (Butland et al., 2005). Bicarbonate is also essential for FAB (Wakil et al., 1958a) as it gets incorporated into malonyl coenzyme A, via biotin carboxylase in the first committed step of FAB and is released later as  $\text{CO}_2$  in a subsequent condensation reaction. Our structure suggests that YchM may sequester ACP to the membrane and provide bicarbonate to the FAB machinery and perhaps also for the biosynthesis of other metabolites including nucleotides, sugars and amino acids (Hillier and Jago, 1978; Merlin et al., 2003). In support of this notion, genome-wide genetic and physical interaction screens showed that YchM interacts functionally and physically with proteins involved in FAB. Furthermore, a deletion strain lacking *ychM* and STAS domain of YchM showed a decrease of incorporation of bicarbonate in the presence of NaCl. Thus, we conclude that YchM, a bacterial member of the SLC26 family of anion transporters, is linked to fatty acid metabolism via a direct interaction with ACP, creating a bicarbonate transport metabolon.

## RESULTS

### Association of STAS Domain of YchM with ACP

In order to determine the structure of the STAS domain of YchM, we constructed an N-terminal hexahistidine ( $\text{His}_6$ )-tagged

small right panel is the representation of a full-length YchM, a 550 amino acid protein including the STAS domain.

(B) The STAS domain of YchM (residues 436–550) bound to ACP are shown in white and blue, respectively. The 4'-PPa is covalently bound to Ser 36 of ACP and is located at the interface between STAS and ACP. All secondary structural elements are illustrated and the N and C termini are labeled.

(C) The surface electrostatic potential of the STAS domain calculated by APBS in complex with ACP illustrates the positively charged regions (blue) interacting with the negatively charged ACP.

(D) The interface between ACP (blue) and the STAS domain (white) is centered around the 4'-PPa and malonyl group that is illustrated within a 2-Fo-Fc electron density map contoured to  $1.8 \sigma$ .

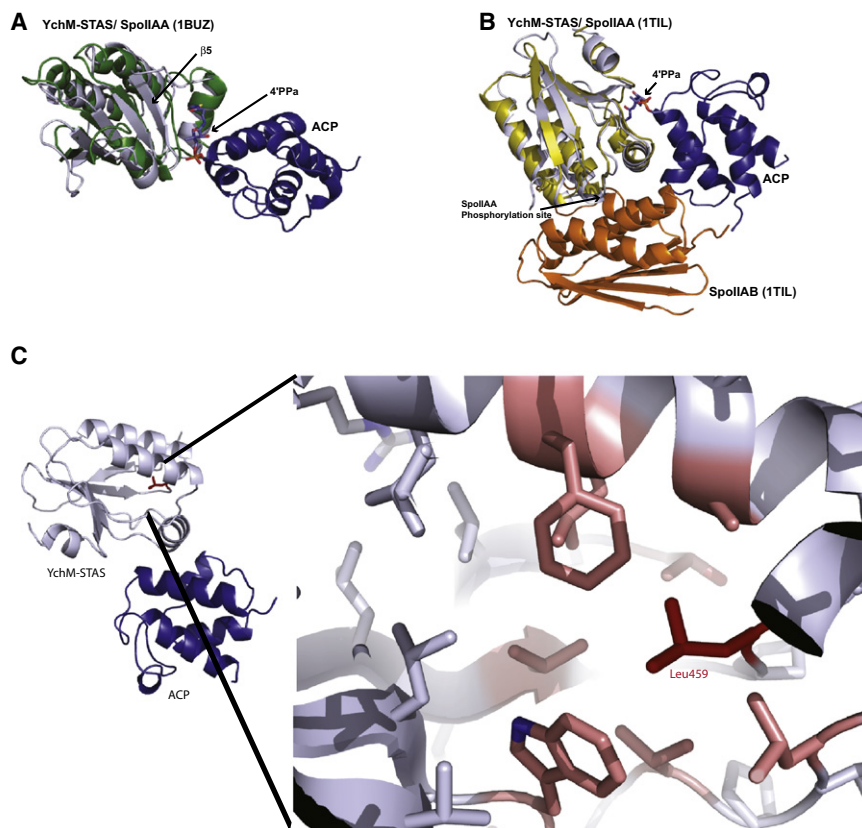


**Figure 2. Structural Homologs of the STAS Domain and Mutants within the SLC26A3 STAS Domains**

(A) The structural overlay of YchM-STAS onto SPOIIAA (pdb accession code: 1BUZ) illustrates the position of the additional fifth  $\beta$  strand on YchM that is created to provide a binding pocket for the malonyl 4'PPa.

(B) The crystal structure of SpoIIAA-SpoIIAB complex (pdb accession code: 1TIL chain D; SpoIIAA is golden and SpoIIAB is orange) superimposed on STAS domain (gray) illustrates that the SpoIIAB kinase has a different binding surface of the STAS domain compared with ACP (blue). The phosphorylation site on SpoIIAA (Phospho-Ser 57) that abrogates binding to SpoIIAB is also shown.

(C) The hydrophobic core of YchM contains residue L459 from the PL\*FFA motif that is highlighted red and residues within 4 Å of Leu459 are highlighted pink with a closeup view inset.

version of the cytosolic STAS domain of YchM with a thrombin cleavage site encompassing residues 436–550 (Figure 1A) and overexpressed the protein in *E. coli* under the control of a T7 inducible promoter. The soluble His<sub>6</sub>-tagged protein was purified by Ni affinity chromatography, followed by proteolytic removal of the N-terminal His<sub>6</sub>-tag and size exclusion chromatography. We found that the STAS domain eluted in two distinct fractions upon size exclusion chromatography; the lower molecular weight fraction contained only the STAS domain and the higher molecular weight fraction contained a second protein with an apparent molecular mass of 18 kDa upon SDS-PAGE (see Figures S1A and S1B available online). Following identification of ACP as the interacting partner by crystallography (see below), immunoblot analysis using rabbit anti-ACP polyclonal antibody confirmed the 18 kDa band as ACP (Figure S1C). In addition, tandem mass spectrometry (LCMS, liquid chromatography mass spectrometry) readily identified YchM in both peak fractions, while ACP was identified in the higher molecular weight fraction (Figure S1D).

#### Structure of the Cytoplasmic STAS Domain of YchM within the STAS-ACP Complex Resembles SpoIIAA

Although unsuccessful in crystallizing the YchM-STAS domain on its own, we were successful at crystallizing the STAS domain of YchM in complex with ACP and solving the crystal structure to high resolution (<2 Å). The structure of the STAS-ACP complex illustrates that the interaction of ACP with STAS is mediated, in part, by the 4-phosphopantetheine (4'-PPa) moiety, covalently attached to ACP (Figures 1B–1D). The STAS domain of YchM

shares 25% sequence identity with sporulation factor SpoIIAA from *Bacillus subtilis* (pdb 1BUZ) (Kovacs et al., 1998) and, based on our structure, it has a similar tertiary fold with an rmsd of 2.4 Å over 93 C-alpha atoms consisting of 4  $\alpha$  helices and 5  $\beta$  strands. The structure of the STAS domain encompasses residues 436–550 of YchM in addition to 3 N-terminal residual residues from the thrombin cleavage site, all of which are visible in the crystal structure. The core STAS domain of YchM consists of four parallel and one antiparallel  $\beta$  strands forming a five-stranded  $\beta$  sheet, flanked by two parallel  $\alpha$  helices, a third  $\alpha$  helix on one face, and a short C-terminal  $\alpha$  helix on the opposite face (Figure 2A). The structure the STAS domain begins with  $\beta$  strand  $\beta$ 1 (R438-P441) antiparallel to the second  $\beta$  strand  $\beta$ 2 (V450-I456) followed by  $\alpha$  helix  $\alpha$ 1 (F461-R474),  $\beta$  strand  $\beta$ 3 (I480-K484),  $\alpha$  helix  $\alpha$ 2 (A493-R505),  $\beta$  strand  $\beta$ 4 (E511-C515),  $\alpha$  helix  $\alpha$ 3 (F519-A528),  $\beta$  strand  $\beta$ 5 (R536-F540), and  $\alpha$  helix  $\alpha$ 4 (R543-A548). In comparison with SpoIIAA, the STAS domain of YchM contains an additional  $\beta$  strand (residues 536–540) onto its core four-stranded  $\beta$  sheet, with residues 532–541 of the YchM STAS domain creating part of a binding pocket to accommodate the 4'-PPa group from ACP (Figure 2A). Plotting the calculated electrostatic potential onto the surface on the STAS domain illustrates a strikingly bimodal charge distribution (Figure 1C) with a positively charged surface within the interaction site with the acidic protein ACP (pI ~3.9) and the opposite surface provides a negatively charged binding region, which could provide a binding surface for a basic protein.

The SpoIIAA coordinates the interactions with its binding partner SpoIIAB through phosphorylation of Ser 57, a residue that is not conserved in YchM (Ala 493) (Figure 2B), showing that Ser phosphorylation at this site does not play a role in YchM function. Furthermore, the potential binding site for the SpoIIAB kinase on SpoIIAA does not overlap with its ACP interaction site on STAS domain of YchM (Figure 2B). This binding

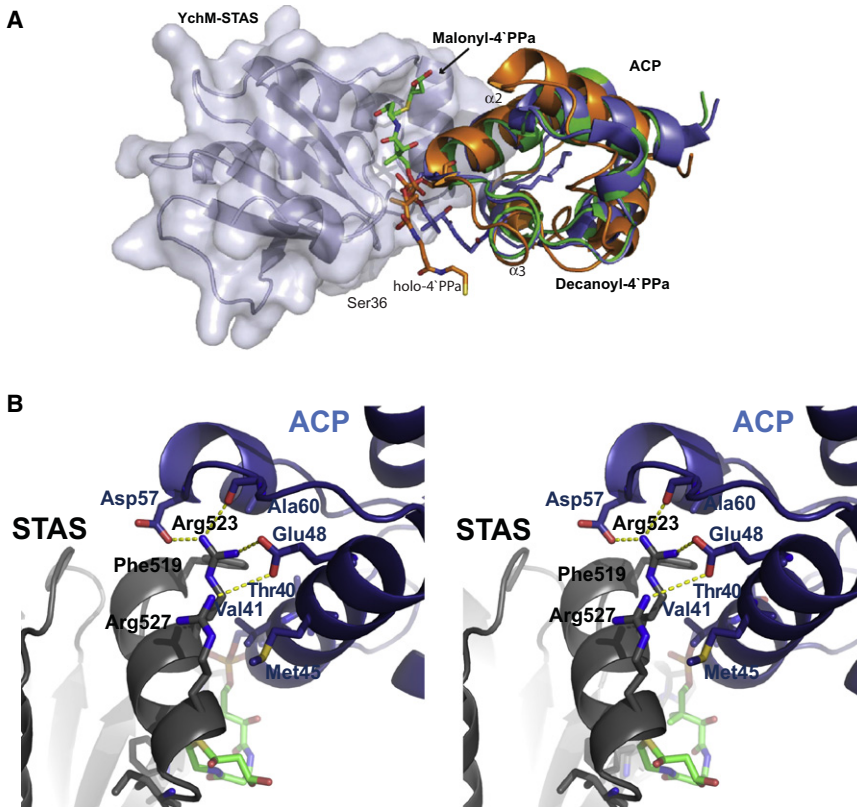


**Figure 3. Structural Overlays of ACPs onto the Complex of YchM-STAS-ACP and YchM-STAS:ACP interface**

(A) Dodecanoyl-ACP (blue, pdb accession code: 2FAE) and 4'PPa-ACP (orange, pdb accession code: 2FQ2) are superimposed onto Malonyl-ACP (green, determined in this study, pdb accession code: 3NY7) in complex with YchM-STAS, to illustrate the different binding locations of the prosthetic group carrying various acyl substrates. (B) A divergent stereo image of YchM-STAS (colored gray) bound to ACP (colored blue) highlights residues within the interface. Residues in the interface and the three key helices are labeled and the 4'PPa group is colored green.

impaired trafficking of these mutants, resulting in loss of cell surface display and transport function in CLD (SLC26A3) or Pendred's syndrome (SLC26A4) patients.

#### Structure of ACP within the YchM STAS-ACP Complex

ACP in complex with the STAS domain contains four  $\alpha$ -helical segments and a large structured loop connects the first and second helices (Figure 1B). The 4'-PPa prosthetic group is attached to Ser36 via a phosphodiester linkage at the N terminus of the second helix (Figures

1B and 1D). The hydrophobic cleft created between helices  $\alpha 2$  and  $\alpha 3$  in ACP provides a flexible binding site for acyl chains of various lengths (Figure 3A) (Roujeinikova et al., 2007). It should be noted that small acyl chains, including those with a negatively charged terminal malonyl group, have a preferred aqueous exposure, while longer hydrophobic chains are bound more tightly to ACP (Roujeinikova et al., 2007). The crystal structure of decanoyl-ACP (2FAE) showed that the extended 4'-PPa group allows the thioester linked decanoyl group to be tucked between helices  $\alpha 2$  and  $\alpha 3$  of ACP (Roujeinikova et al., 2007).

#### Insights into the STAS Domain and Human Disease

The STAS domain of the SLC26 family has significant roles in mammalian cells. Congenital chloride-losing diarrhea (CLD) is a genetic disorder causing watery stool and dehydration (Dorwart et al., 2008a). A mutation within the STAS domain (I544N) of the SLC26A3 transporter leads to retention in the endoplasmic reticulum and loss of functional expression (Mäkelä et al., 2002). The relevant I544N mutation can be mapped to residue L459 within the conserved segment PI\*YFA in human SLC26A3 which is PL\*FFA in YchM located within the hydrophobic core of the STAS domain of YchM (Figure 2C; Figure S2). Furthermore, a naturally occurring mutation in STAS domain of SLC26A4 (pendrin) (L676Q) leads to Pendred's syndrome (Gillam et al., 2004). The equivalent Phe499 in the STAS domain of YchM is located centrally on helix  $\alpha 2$  with its side chain oriented within the hydrophobic core (Figure S2). Putting an unfavorable polar Asn or Gln into the hydrophobic pocket of the STAS domain may lead to destabilization of the STAS domain, misfolding, and subsequent

Overall, the structure of ACP in complex with the STAS domain resembles the apo form of ACP (1T8K rmsd 0.56 Å using all 77 backbone C-alpha atoms) as determined by X-ray crystallography rather than holo-ACP conjugated to hexanoyl and decanoyl acetyl groups (2FAC-rmsd 0.89 Å and 2FAE-rmsd 0.87 Å using all 77 backbone C-alpha residues) (Roujeinikova et al., 2007; Wu et al., 2009). This makes sense as the prosthetic group attached to ACP does not occupy the hydrophobic cleft of ACP. Within the STAS-ACP structure, the 4'-PPa is flipped 180° around the phosphate group and is exposed on the opposite surface of ACP, at the interface of the STAS with ACP (Figure 1D). NMR structures of apo, holo, and butyryl forms of *E. coli* ACP (Wu et al., 2009) suggest that the differences in the electrostatic surface properties of the different ACP derivatives, especially on helix  $\alpha 3$ , lead to specific binding determinants as helix  $\alpha 3$  undergoes subtle conformational changes when ACP is bound with acyl chains. In the complex, the surface of ACP helix  $\alpha 3$  is critical to the interaction with STAS as illustrated in our structure of the STAS ACP complex.

The interaction between the STAS domain and ACP involves the surface exposed regions of the  $\alpha 2$  and  $\alpha 3$  helices from ACP surrounding the aforementioned  $\alpha 3$  helix of the STAS domain from YchM (Figure 1B). This interface buries a total of 850 Å<sup>2</sup> of surface area, including several hydrogen bonds between the side-chain amide of Arg 523 (STAS) and the carboxyl groups of Glu 48 and Asp 57 and the carbonyl backbone of Ile 55 from ACP. The side-chain amide of Arg 527 (STAS) also makes a salt bridge with Glu 48 of ACP (Figure 3B). There are several hydrophobic interactions centered around residue Phe 519 of STAS that protrudes into the hydrophobic pocket containing residues Ala 60, from helix  $\alpha 3$  of ACP, and Thr 40 and Val41 from helix  $\alpha 2$  of ACP. In addition, Met 45 of ACP makes Van der Waals contacts with Arg 527 (Figure 3B).

#### YchM Makes Direct Contact with the Thiol Ester Linked Malonyl Group and 4'-PPa Prosthetic Group on ACP

The interaction between STAS and ACP also involves the 4'-PPa group that is covalently attached to the side-chain hydroxyl of Ser 36 of ACP. The 4'-PPa group sits in a pocket created between the  $\alpha 3$  helix and the  $\beta 5$  strand found in the STAS domain of YchM and buries an additional 240 Å<sup>2</sup> of surface area (Figure 1C). Several residues of the STAS domain located in this region make direct contact with the 4'-PPa group, including Phe 539 that forms the basis of a hydrophobic pocket that includes residues Phe 540, Pro 532, Pro 541, and Ile 530 (Figure 1D). The backbone carbonyl of YchM Phe 539 makes a water-mediated hydrogen bond with O13 of the 4'-PPa group and its amide nitrogen also makes an H-bond with the O18 of the 4'-PPa. Upon inspection of difference density (Fo-Fc) maps at the end of the 4'-PPa group, there is density for a terminal malonyl group, an intermediate in the FAB pathway. The carboxyl group of the malonyl makes H-bonds with the side chain of YchM-STAS Gln 531 (Figure 1D). Thus, the STAS domain of YchM interacts with malonyl-ACP, the activated intermediate in acylation reactions, such as those involved in FAB.

#### YchM Interacts Genetically with the FAB Pathway

In order to independently assess the functional connection between YchM and FAB, a genome-wide genetic screen was performed. Genetic suppression and synthetic lethal analyses are one of the most informative methods for discovering functional relationships among bacterial genes (Babu et al., 2009b). In particular, aggravating functional genetic relationships are conveyed by the slow growth or inviability of the double mutants relative to the single deletion growth phenotypes, implying that the genes are in related (i.e., parallel) pathways that converge on a common cellular process (i.e., functional redundancy), while alleviating genetic interaction between two genes are usually interpreted in terms of similarity (same pathway) of function (Babu et al., 2009b). Thus, we applied a high-throughput *E. coli* Synthetic Genetic Array (eSGA) screening approach, recently devised by our group (Butland et al., 2008), to identify *E. coli* genes that interact genetically with strains deleted entirely for *ychM* or only its STAS domain (Figure 1A). We generated double mutants by conjugating *ychM* $\Delta$  or *STAS* $\Delta$  strains (marked with  $\Delta::Cm^R$ ) with single gene deletions of almost all other non-essential *E. coli* genes, as well as potentially hypomorphic alleles of selected essential *E. coli* genes (marked with  $\Delta::Kan^R$ ). The

colony sizes of the *ychM* $\Delta$  or *STAS* $\Delta$  double mutants surviving dual drug selection were then quantified by digital imaging. Using a statistical interaction score (S) to quantify both the strength and confidence of interactions for each *E. coli* mutant gene pair (Table S1A), we detected cases of both synthetic sickness or lethality (SSL) (i.e., negative or aggravating interactions) and alleviating (i.e., positive or suppressing) growth phenotypes. Overrepresentation analysis using Gene Ontology (GO) annotation terms showed that the interacting genes identified in the *ychM* $\Delta$  and *STAS* $\Delta$  deletion screens were enriched significantly (q-value < 0.05) (see Supplemental Experimental Procedures) for genes linked to fatty acid metabolism, lipid and lipopolysaccharide biosynthetic process, chromosome segregation, transporters, as well as other processes linked to membrane, translation, and cellular metabolism (Tables S1B and S1C). This suggests that YchM may be part of a large network of interacting proteins involved in FAB and other metabolic process.

As was the case for the structural experiments, we also observed genetic interactions of *ychM* $\Delta$  and/or *STAS* $\Delta$  with deletions of several FAB pathway genes. These included SSL interactions with a hypomorphic allele of ACP (*acpP*), and with partially inactivated allele of a gene mediating the acetyl-CoA carboxylation reaction (*accD*), as well as genes mediating the condensation (*fabD* and *fabB*) and subsequent elongation reactions (*fabA*, *fabG* and *fabI*) (Figure 4A; Figure S2A and Table S1A) through which fatty acid biosynthesis in *E. coli* takes place (Magnuson et al., 1993). Malonyl-ACP is the product of malonyl-CoA-ACP transacylase, the product of the *fabD* gene. It is not surprising that FabD has a strongly aggravating genetic interaction with YchM and STAS deletions (Figure 4) as malonyl-ACP is the metabolic intermediate detected in complex with YchM-STAS. Malonyl-ACP is also a substrate for acetoacetyl-ACP synthase the *fabB* gene product (Figure S3).

The *ychM* $\Delta$  and/or *STAS* $\Delta$  eSGA screens also identified aggravating interactions with mutations of individual fatty acid degradation (*fad*) regulon pathway components (*fadADEHJIR*) responsible for the transport, activation, and  $\beta$ -oxidation of medium (C<sub>7</sub> to C<sub>11</sub>) and long (C<sub>12</sub> to C<sub>18</sub>) chain fatty acids (Figure S3B). The Fad regulon genes are largely controlled by the *fadR* gene product (Feng and Cronan, 2009; Magnuson et al., 1993). In *E. coli*, *fadR* has dual functions as both repressor of the  $\beta$ -oxidation pathway and activator of the FAB pathway genes (Henry and Cronan, 1991). Interestingly, the *ychM* $\Delta$  deletion mutant also showed an SSL interaction with a new member of the Fad regulon, *fadM* (*ybaW*) (Figure S3A), which has been shown to be regulated by FadR and encodes a thioesterase capable of cleaving the thioester bonds of inhibitory acyl-coenzyme A (CoA) during oxidation of unsaturated fatty acids (Feng and Cronan, 2009; Nie et al., 2008). Thus, YchM may play a role in the regulation of fatty acid metabolism, perhaps acting as part of a sensor system for bicarbonate.

We confirmed the reliability of the whole genome interactions we identified for *ychM* $\Delta$  and *STAS* $\Delta$  with FAB pathway genes by using custom mini-arrays (see Supplemental Data). In each case, we conjugated donor Cm<sup>R</sup>-marked strains harboring the deleted *ychM* $\Delta$  and *STAS* $\Delta$  genes with recipients containing Kan<sup>R</sup> marked deletion or potentially hypomorphic alleles of *fabABDGI*, *fadADEHJIRM*, *acpP*, *accA*, and *accD*, and unrelated genes outside the *fab*, *fad*, *acpP*, *accA*, and *accD* genes. Consistent

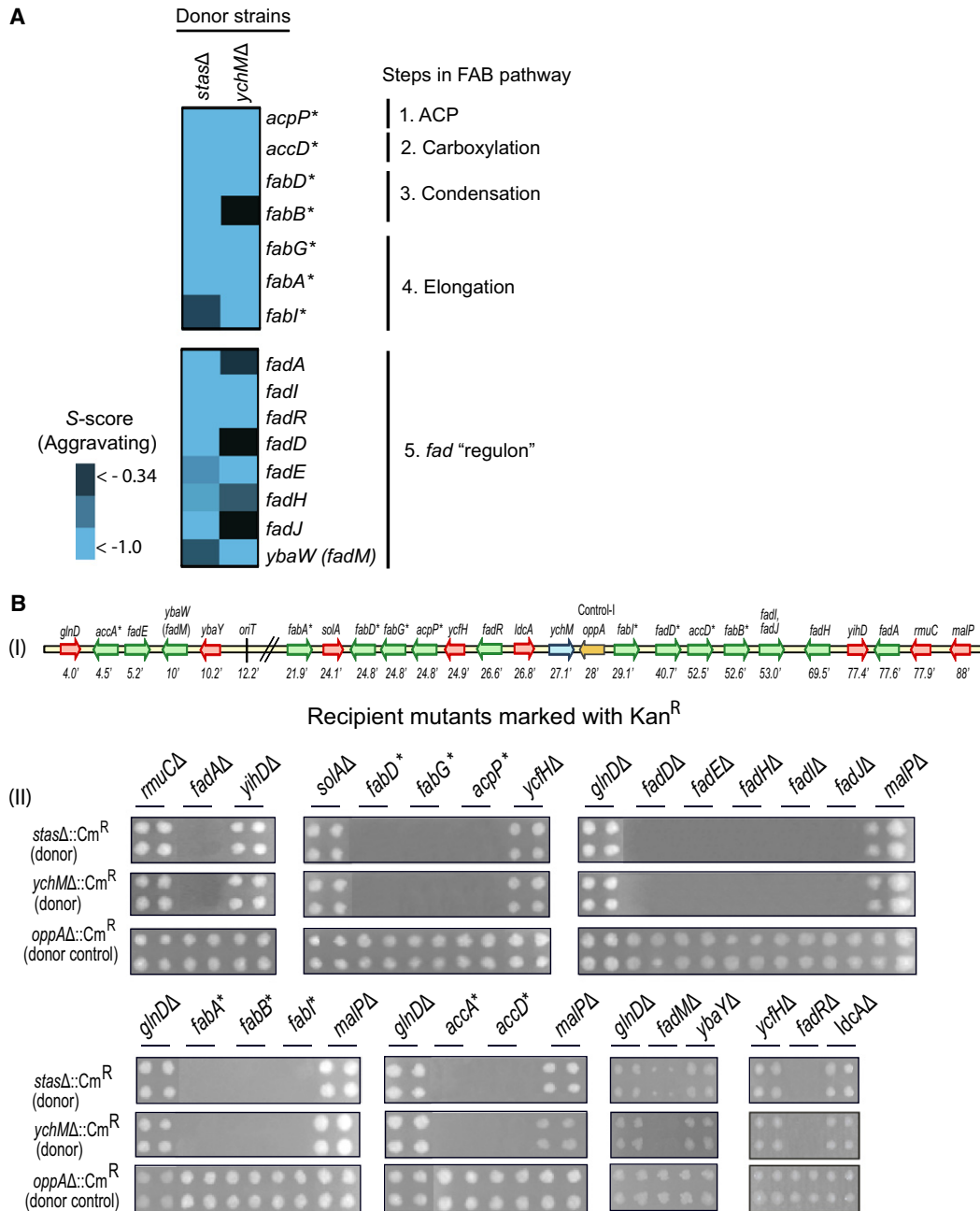


**Figure 4. Genetic Interactions of *ychMΔ* and *STASΔ* with Genes Involved in the Fatty Acid Biosynthesis Pathway**

(A) Aggravating genetic interactions of *ychMΔ* and *STASΔ* with genes involved in the various steps of the fatty acid biosynthesis pathway are shown. Blue represents aggravating (negative S score) interaction. Asterisks represent essential alleles.

(B) Chromosomal positions of *ychM* (blue arrow), *fadADEHIJMR*, *fabABDGI*, *acpP*, *accA* and *accD* (green arrows), and other gene (red arrows) deletions used as donors (marked with Cm<sup>R</sup>) or recipients (marked with Kan<sup>R</sup>) in eSGA experiments are shown in (I). *oppA* donor deletion (orange arrow) located close to the *ychM* gene served as control for effects of proximity on recombination. The numbers indicate the gene coordinates on the *E. coli* chromosome (in minutes). *oriT* is the F origin of transfer in Hfr Cavalli (12.2 min). In (II), *ychMΔ*, *STASΔ* and control (*oppAΔ*) donor deletion strains were crossed with recipients containing Kan<sup>R</sup> marked deletion or potentially hypomorphic alleles of *fabABDGI*, *fadADEHIJMR*, *acpP*, *accA*, and *accD*, or various unrelated genes flanking *fadADEHIJMR*, *fabABDGI*, *acpP*, *accA*, and *accD* genes, followed by selection on plates containing chloramphenicol and kanamycin. The essential gene *accA*, not included as part of the recipient knockout library collection, is constructed separately to confirm the genetic interaction of *ychMΔ* or *STASΔ* with *accA*. Asterisks represent essential alleles.

with our *ychMΔ* and *STASΔ* whole-genome screens, the individual recipient deletion alleles of the *fabABDGI*, *fadADEHIJMR*, *acpP*, *accA*, and *accD* exhibited the expected SSL phenotypes

when combined with *ychMΔ* and *STASΔ* donor deletion strains (Figure 4B). These genetic interactions were not a consequence of recombination suppression resulting from gene proximity

because no noticeable effects on growth were observed when *ychM* $\Delta$  or *STAS* $\Delta$  donor deletions were combined with deletions of functionally unrelated genes flanking the *fab*, *fad*, *acpP*, *accA*, and *accD* genes. Additionally, the use as donor of another unrelated gene in the same region as *ychM*, namely *oppA*, did not reveal synthetic genetic interaction with *fabABDGI*, *fadADEH-JIRM*, *acpP*, *accA*, and *accD* genes (Figure 4B). Clearly, YchM has synthetic lethal interactions with genes involved in FAB within *E. coli*.

### YchM Associates Physically with Proteins Implicated in the Fatty Acid Metabolism

Our structural and genetic data pointed to a role of YchM in FAB. Therefore, we performed an unbiased protein interaction screen to identify its physical interaction partners in vivo. Full-length YchM was affinity-tagged at its C-terminal end by recombining a SPA (Sequential Peptide Affinity) cassette (consisting of a triple FLAG tag and a calmodulin binding peptide) into the chromosome (Butland et al., 2005). SPA-tagged YchM was extracted from the membranes of log-phase cultures using three different detergents (Triton X-100, DDM [n-dodecyl- $\beta$ -D-maltopyranoside], and C<sub>12</sub>E<sub>8</sub> [Octaethylene glycol monododecyl ether]) at 1% concentrations, following which the stably associated proteins were affinity-purified in two steps on anti-FLAG and calmodulin resins and then identified using tandem mass spectrometry (LCMS) and peptide mass fingerprinting (MALDI-TOF MS). Three preparations with different detergents were used (Díaz-Mejía et al., 2009) in order to optimize the solubilization and partly validate interacting proteins.

Among the proteins copurifying with YchM were 14 proteins functioning in transport, energy, membrane biogenesis, and FAB and FAD (Figure 5A; Table S2 and Supplemental Experimental Procedures). The last group included: FabA, FabR, FadE, and FadJ, which are the major players in the FAB and FAD pathways. Interactions with FAB and FAD pathway components FabA, FabR, FadE, and FadJ are likely to be meaningful because each was detected in purifications of YchM with at least two different detergents with high spectral peptide counts (Figure 5B). The physical associations of YchM with FadE, that encodes acylCoA dehydrogenase, were additionally validated by coimmunoprecipitation in strains containing endogenously expressed C-terminal affinity-tagged FadE and overexpressed C-terminal His<sub>6</sub>-tagged YchM. The FadE affinity tagged protein was immunoprecipitated from the cell lysates and the presence of YchM was probed by immunoblot using anti-His monoclonal antibody (Figure 5C). As expected, in the presence of 0.5 mM IPTG induction, YchM coprecipitated with tagged FadE but not with a C-terminal YgbT tagged control protein unrelated to FAB (Figure 5C). Thus, there is a stable physical association of the *E. coli* YchM with FadE protein implicated in FAD pathway. FadE was also identified as an aggravating genetic interaction (Figure 4). Although other FAB and FAD pathway proteins copurified in purifications of YchM with at least two different detergents, the specificity of these interactions was not tested.

Despite our copurification and cocrystallization of the overexpressed STAS domain of YchM with ACP, we were, surprisingly, unable to detect a YchM-ACP interaction following the purification of YchM expressed from its chromosomal location with

a C-terminal SPA-tag or His<sub>6</sub>-tag. The failure may have reflected (1) inefficient fragmentation and identification of ACP, a small protein, by mass spectrometry, (2) interference of ACP binding by the C-terminal tags on YchM, or (3) the relatively low abundance of YchM as reflected by its low codon adaptation index and low mRNA expression level in *E. coli* (Hu et al., 2009). In order to verify the interaction of YchM with ACP, we overexpressed YchM with a C-terminal His<sub>6</sub>-tag and purified YchM from whole cells solubilized directly using the detergent C<sub>12</sub>E<sub>8</sub>. The purified fractions were then analyzed by immunoblot using anti-ACP antibody. We were able to detect ACP in the purified YchM fractions; however the bulk of ACP was in the soluble fraction as expected for this abundant cytosolic protein (Figure 5D).

### Effect of YchM Deletions on Bicarbonate Incorporation and on Cell Growth

As a bacterial member of the SLC26 family of anion transporters, YchM may transport anions like bicarbonate across the *E. coli* inner membrane. In order to determine whether *E. coli* YchM can mediate bicarbonate uptake, we performed bicarbonate incorporation assays on wild-type *E. coli* and on strains deleted for *YchM* or its *STAS* domain in an isogenic strain background, at alkaline pH, in the presence and/or absence of NaCl. All strains were able to incorporate [<sup>14</sup>C] bicarbonate into acid-stable material, showing that bicarbonate can enter *E. coli*, in the absence of YchM, perhaps as diffusible CO<sub>2</sub> (Kozliak et al., 1995) or by another protein-mediated pathway that has been proposed for CO<sub>2</sub> transport via aquaporins (Endeward et al., 2006; Prasad et al., 1998) or the ammonia transporter (Musa-Aziz et al., 2009). We observed a 2.7-fold increase in [<sup>14</sup>C] bicarbonate incorporation in wild-type *E. coli* in the presence of 100 mM NaCl relative to the incorporation in the absence of NaCl after 1 hr incubation at room temperature at alkaline pH 8.3 (Figure S6A). Conversely, only a blunted 2.0- and 1.6-fold increase in bicarbonate incorporation was observed in *ychM* and *STAS* deletion strains under identical experimental conditions (Figure S6A). Figure S6B shows the time dependence of [<sup>14</sup>C] bicarbonate incorporation in the wild-type and in two deletion strains after subtraction of the incorporation in the absence of NaCl. Only wild-type *E. coli* showed a time-dependent increase in bicarbonate incorporation over the 1 hr time period. These results suggest that YchM is an anion transporter as expected for the SLC26 family that can facilitate bicarbonate (or carbonate) transport in the presence of NaCl. A full characterization of the transport properties of YchM, including its substrate specificity, pH and ion dependence, and its kinetics and regulation will require further studies using purified, reconstituted protein.

When *ychM* and *STAS* deletion mutants along with the wild-type were assayed for their growth at three different pH conditions (pH 4.0, 7.0, and 8.3), both the *STAS* and *ychM* deletion strains exhibited a dramatic ~13-fold reduced growth for a period of 48 hr at pH 8.3 compared with the wild-type cells (Figure S4). Nonetheless, log phase growth of the deletion mutants and the wild-type cells were not significantly affected at pH 4.0 and 7.0, respectively in LB-rich media. These results suggest that YchM is an essential gene for *E. coli* growth under alkaline conditions, perhaps related to bicarbonate/carbonate transport activity.

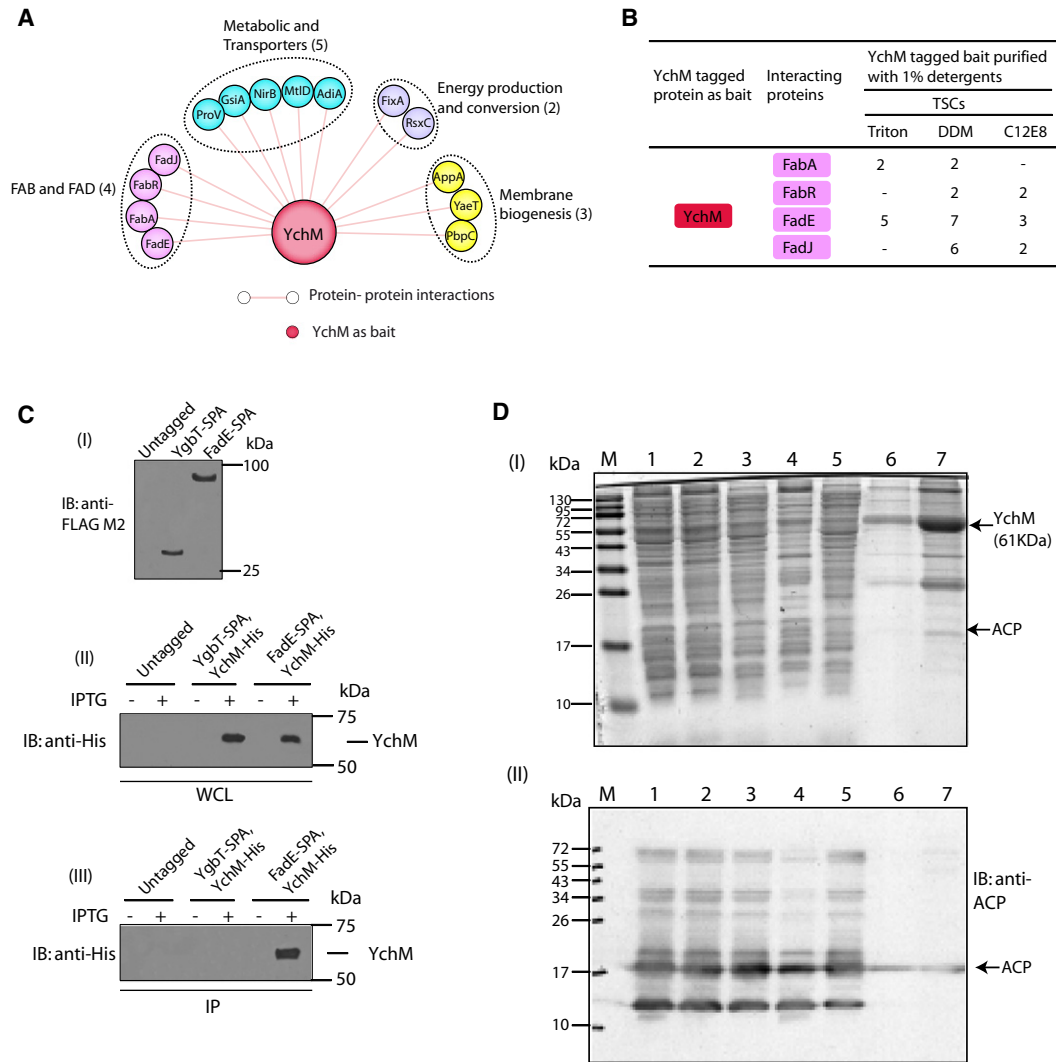


**Figure 5. Physical Interactions of YchM with FAB and with Other *E. coli* Proteins**

(A) Proteins involved in various biological processes, including FAB proteins that copurified with C-terminally SPA-tagged YchM are indicated and organized according to COG functional groups. Red node represents tagged protein used as bait. Pink edges represent protein-protein associations identified by mass spectrometry.

(B) Identification of FabA, FabR, FadE, and FadJ proteins by LCMS from the C-terminally SPA-tagged YchM purified protein that were consistently appeared in more than two different detergents, and their probability scores and total spectral counts (TSCs) are shown in a table for easier visualization.

(C) Coimmunoprecipitation of YchM with FadE protein. (I) Immunoblot (IB) analysis on the expression of the SPA-tagged non-fatty acid, YgbT and fatty acid, FadE strains using M2 anti-FLAG antibody. The untagged parental C41 (DE3) strain served as control. The non-fatty acid YgbT SPA-tagged strain served as a second control. (II and III) IB analysis of the whole-cell lysates (WCL, II) and anti-FLAG immunoprecipitates (IP, III) from the *E. coli* C41 (DE3) strain expressing a SPA-tagged YgbT or FadE with His<sub>6</sub>-tag YchM probed with anti-His monoclonal antibody. Molecular masses of marker proteins on the SDS-polyacrylamide gel are indicated in kDa. See [Supplemental Experimental Procedures](#) for details.

(D) Copurification of ACP with YchM protein. (I) Coomassie blue stained SDS-PAGE gel (16%) of the YchM solubilized with the mild non-ionic detergent C<sub>12</sub>E<sub>8</sub> from whole-cell lysates. Lane 1, total expression of YchM protein after french press; Lane 2, total cell extract from YchM with C<sub>12</sub>E<sub>8</sub> detergent; Lane 3, soluble supernatant fraction with C<sub>12</sub>E<sub>8</sub>; Lane 4, insoluble pellet with C<sub>12</sub>E<sub>8</sub>; Lane 5, flow-through from Ni-NTA column; Lane 6, flow-through from the last washing step prior to YchM elution; and Lane 7, flow-through of the second elution from the Ni-NTA binding. (2) Immunoblot (IB) analysis of the fractions, shown as in (1), using anti-ACP antibody illustrating ACP running as a ~18 kDa band. Molecular masses of marker proteins on the SDS-PAGE gel are indicated in kDa.

## DISCUSSION

Little is known about the function of YchM in *E. coli* other than it is a member of the SLC26 family of anion transporters. Our structural analysis provided the first crystal structure of a bacterial STAS domain, illustrating similarity to SpoIIAA (the soluble

bacterial antisigma factor antagonist), but with an additional strand and loop features on YchM to accommodate its binding partner ACP. SpoIIAA had been crystallized in complex with SpoIIAB and this site of interaction is located on a surface distinct for the YchM-ACP interaction site. This suggests that STAS domains can function to mediate multiple specific protein

interactions beyond ACP. The YchM STAS domain structure serves as a model for other anion transporter STAS domains. The structure based homology models account for structural mutations that result in human diseases such as CLD (Figure 2C). The STAS domains from human SLC26 transporters have been difficult to crystallize and we were unable to crystallize the STAS domain of YchM on its own, perhaps in part because STAS domains have intrinsically disordered regions in the absence of binding partners, a common theme in many signaling proteins (Mittag et al., 2010). Our cocrystal structure showed a specific interaction between the cytosolic domain of YchM (STAS) and ACP, suggesting that the STAS domain of YchM in *E. coli* could play a role in sequestering ACP to the inner membrane, the site of phospholipid biosynthesis.

In order to probe for such a cellular role for YchM and to determine what role the STAS domain plays in YchM's function (especially with respect to mediating FAB), we used eSGA approach (Butland et al., 2008) to identify *E. coli* genes interacting genetically with deletion mutants of *ychM* (deletion of full-length *ychM* including its STAS domain) or *STAS* (deletion within *ychM*). We confirmed SSL interactions of *ychM* or *STAS* deletion mutants with a hypomorphic allele of ACP (*acpP*), and with partially inactivated allele of a gene mediating the acetyl-CoA carboxylation reaction (*accD*), as well as genes mediating the condensation (*fabD* and *fabB*) and subsequent elongation reactions (*fabA*, *fabG*, and *fabI*) (Figure 4A; Figure S3A and Table S1A) through which fatty acid biosynthesis in *E. coli* takes place (Magnuson et al., 1993). The *ychM* $\Delta$  and/or *STAS* $\Delta$  eSGA screens also identified aggravating interactions with mutations of individual *fad* regulon pathway components (*fadADEHJIR*). This interaction likely plays a regulatory role linking bicarbonate transport and fatty acid biosynthesis.

The two most important cofactors in FAB are coenzyme A (CoA) and ACP, which carries the growing acyl chain from one enzyme to another by supplying precursors for the condensation reactions. These precursors are derived from the acetyl-CoA pool. Malonyl-CoA is required for the elongation steps and is formed by the first committed step in FAB synthesis, acetylCoA carboxylase (*accD*). Malonyl-ACP is the product of the reaction of malonyl-CoA:ACP transferase, encoded by the *fabD* gene, and is a substrate for the  $\beta$ -keto-ACP synthases I-III, encoded by the *fabB* gene (Figure S3A). Within our heterodimeric structure of STAS bound to ACP, we see the carboxyl group of the malonyl-CoA (4'PPA) making a hydrogen bond with the side chain of YchM-STAS Gln 531 (Figure 1D). Malonyl-ACP is the activated donor form of acetyl groups that participate in the condensation reaction, one of the reaction steps in the FAB pathway. Thus, the STAS domain interacts with an activated acetyl-ACP intermediate, suggesting that YchM could act as a sensor for the state of flux through the FAB and other ACP-dependent pathway, perhaps regulating bicarbonate transport.

The *ychM* $\Delta$  and *STAS* $\Delta$  eSGA screens also identified aggravating interactions outside of the FAB system, including ones with lipoproteins (*loIABCDE*), D-alanine-D-alanine ligase A (*ddlA*), the D-Ala-D-Ala membrane component of ABC transporters (*ddpBCDFX*), and the membrane-bound ATP synthase (*atpCDEFGH*) (Table S1A). The observed interactions of some of these genes with *ychM* $\Delta$  and *STAS* $\Delta$  are likely repercussions of the perturbation to fatty acids in phospholipids that are essen-

tial for the translocation of lipoproteins into the outer membrane of *E. coli* and for their subsequent assembly into the murein sacculus (e.g., *ddlA*) (Wu et al., 1980). In addition, energy derived from the membrane-bound ATP synthase is consumed by acyl transferases during conversion of fatty acid to acyl-ACP (Magnuson et al., 1993). Conversely, the interaction with the D-Ala-D-Ala membrane component of ABC transporters suggests that YchM might be important in the translocation of diverse substrates across the cell membrane.

Independent of our structural studies, we also screened genome wide for proteins that physically interact with YchM. In the YchM affinity purification, we detected proteins within the FAB and FAD pathways including FabA, FabR, FadE, and FadJ. We confirmed through coimmunoprecipitation that YchM forms a stable physical association with FadE, and our genetic interaction study suggest that, indeed, it functions in fatty acid biosynthesis in cooperation with FadE. It is also possible that the other copurifying proteins may be associated with YchM through ACP or via other available sites on the STAS domain or the membrane domain. Based on our structure of the YchM-STAS, it is likely that YchM interacts with additional proteins, such as those involved in FAB, while interacting with ACP via an exposed binding site on the STAS domain that is utilized by structural homologs of the STAS domain, SpoIIAA, to bind regulatory proteins.

The structure of the YchM cytosolic STAS domain bound to ACP provided the basis for predicting a functional role for YchM. Our results from genetic and physical interactions show that YchM plays a role in fatty acid metabolism. In *E. coli*, bicarbonate is used as an essential metabolic substrate for fatty acid biosynthesis during normal growth, as well as for carboxylation reactions during the synthesis of various small molecules including nucleotides and amino acids (Merlin et al., 2003; Wakil et al., 1958b). YchM may act as a bicarbonate/carbonate transporter that sequesters fatty acid synthase enzymes on the inner membrane to create a transport metabolon (Reithmeier, 2001) that channels external bicarbonate directly into FAB (Figure 6C) specifically to acetyl-CoA carboxylase (*AccA*), the first committed enzyme of de novo fatty acid synthesis (Wakil et al., 1958b). Since the STAS domain interacts with the metabolic intermediate malonyl-ACP, YchM could act as a regulator for flux through the FAB pathway or as part of a sensor system for external pH or bicarbonate. Clearly, the STAS domain of YchM is involved in mediating specific protein interactions. The STAS domain of other members of the SLC26 family likely have a similar function and the identification of their interacting proteins may reveal how these anion transporters participate in other cellular functions.

## EXPERIMENTAL PROCEDURES

### Histidine Tagging and Purification of STAS Domain of YchM

The N-terminal hexahistidine-tagged STAS domain of YchM protein was over-expressed and purified using metal affinity chromatography as described in the Supplemental Experimental Procedures.

### Protein Crystallization, Structure Determination, and Refinement

Both the YchM STAS domain and the isolated complex for protein crystallization, structure determination, and refinement of the crystals were described in the Supplemental Experimental Procedures. The data collection, SAD

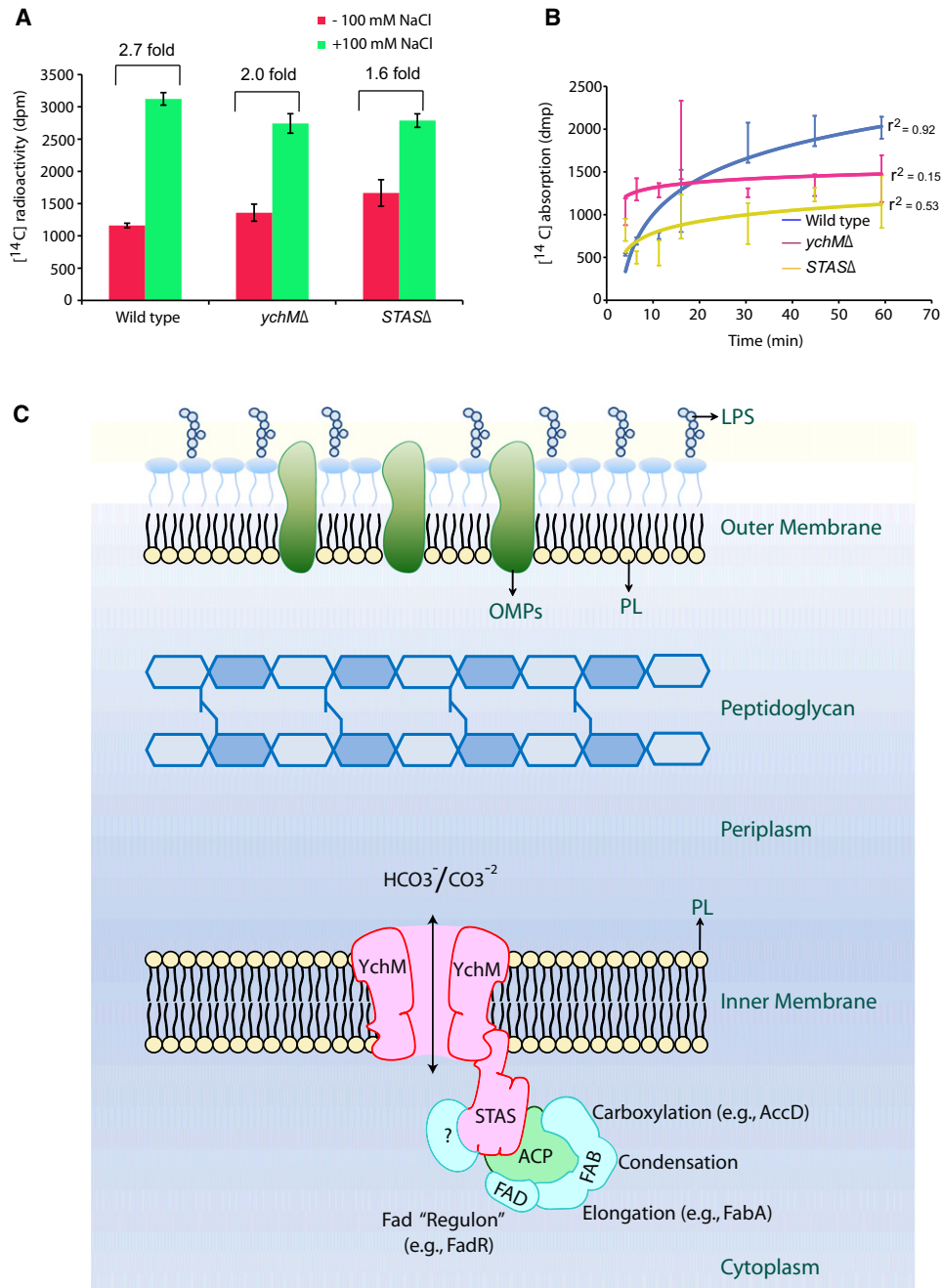


**Figure 6. Uptake of Bicarbonate by YchM and a Proposed Functional Role for YchM in the FAB Pathway**

(A) Uptake of bicarbonate incorporation in the wild-type and *ychMΔ* or *STASΔ* deletion stationary phase cells were measured in the presence and absence of 100 mM NaCl. Bicarbonate uptake was determined by  $^{14}\text{C}$  accumulation in cells after 1 hr as measured by liquid scintillation counting. Data was obtained from three independent cultures and error bars represent standard deviation from the mean. See Supplemental Experimental Procedures for details.

(B) The time dependence of sodium dependent bicarbonate (or carbonate) incorporation in the wild-type and *ychMΔ* or *STASΔ* deletion cells grown in LB medium subtracting uptake into cells without added NaCl were measured. Bicarbonate uptake rates were determined by acid stable  $^{14}\text{C}$  accumulation in cells as measured by liquid scintillation counting at times indicated.

(C) The proposed role of YchM with ACP and with members of the FAB pathway (carboxylation, condensation and elongation) is shown based on the evidence gathered from structural, genetic, physical and functional interaction studies. AccD and FabA are shown as examples of the carboxylation and elongation steps within the FAB pathway, respectively. YchM embeds in the inner membrane of *E. coli* with a C-terminal STAS domain is located in the cytoplasm. The “?” interaction with STAS refers to the ability of STAS to interact with ACP on a surface that is independent of a protein-protein interaction surface that has been shown on a homologous STAS protein to bind SpoIIAB (an antisigma factor) (Figure 2). Therefore, it is possible that STAS is able to interact with ACP as well as with other unknown proteins at the same time. Since YchM is an anion transporter it is likely to play a role in supplying bicarbonate to AccD in the first committed step in FAB pathway. In addition, STAS may act as a regulator of bicarbonate uptake and the flux through the FAB pathway by sensing the FAB intermediate malonyl-ACP and/or by sensing extracellular bicarbonate or pH, thereby regulating growth at alkaline pH. PL, phospholipids; LPS, lipopolysacchride; OMPs, outer membrane proteins.

**Table 1. Data collection, SAD Phasing, and Refinement Statistics for YchM-STAS in Complex with ACP**

	Native	NaI Soak
Data collection		
Space group	P2 <sub>1</sub> 2 <sub>1</sub> 2 <sub>1</sub>	P2 <sub>1</sub> 2 <sub>1</sub> 2 <sub>1</sub>
Cell dimensions		
a, b, c (Å)	33.6, 55.9, 113.4	33.8, 55.9, 113.3
α, β, γ (°)	90 90 90	90 90 90
		<i>Peak</i>
Wavelength	1.54	1.54
Resolution (Å)	50–1.92 (1.99–1.92)	50–2.4 (2.48–2.40)
R <sub>sym</sub> or R <sub>merge</sub>	0.058 (0.35)	0.094 (0.33)
I / σI	26.6 (3.9)	25.7 (4.1)
Completeness (%)	98.0 (81.8)	94.5 (65.9)
Redundancy	5.2 (3.2)	8.6 (3.6)
Refinement		
Resolution (Å)	39.8–1.92	
No. reflections	15139	
R <sub>work</sub> / R <sub>free</sub>	0.1633/0.2190	
No. atoms	1772	
Protein	1513	
Ligand/ion	27	
Water	232	
B factors	21.49	
Protein	20.21	
Ligand/ion	24.18 (glycerol) 20.8 (PPa)	
Water	29.98	
Rmsd		
Bond lengths (Å)	0.008	
Bond angles (°)	1.069	

Values in parentheses are for highest resolution shell.

phasing, and refinement statistics for YchM-STAS in complex with ACP is shown in Table 1.

#### Genome-wide *E. coli* Synthetic Genetic Array (eSGA) Screen

A full-genome eSGA screen using *ychMΔ::Cm<sup>R</sup>* and *STASΔ::Cm<sup>R</sup>* deletions in Hfr Cavalli (Hfr C) as donor was carried out and analyzed as previously described (Butland et al., 2008), as were various miniarray crosses. Interaction scores (S) were calculated as previously described (Butland et al., 2008) to quantify the strength and confidence of the genetic interaction for each mutant gene pair.

#### Endogenous YchM Affinity Tagging and Purification

The YchM protein was C-terminally tagged using a sequential peptide affinity (SPA) dual tagging system as previously described (Babu et al., 2009a), except in all purification steps mild nonionic detergents –1% Triton, or 1% DDM or 1% C<sub>12</sub>E<sub>8</sub>, was added to disrupt the association of YchM with the membrane fraction. The analysis of mass spectrometry data was essentially performed as previously described (Babu et al., 2009a).

#### Overproduced YchM Histidine Tagging and Purification

Full-length YchM was cloned into a pET41b plasmid with a kanamycin selectable marker containing a C-terminal thrombin cleavable 6xHis tag under the control of a T7 promoter. The details of YchM histidine tagging and purification are shown in Supplemental Experimental Procedures.

#### Coimmunoprecipitation, Sodium Bicarbonate Incorporation, and pH Growth Curve Assays

The physical interaction of YchM with FadE was confirmed using coimmunoprecipitation, sodium bicarbonate incorporation, and pH growth assays in wild-type (Hfr C) and the *ychM* and *STAS* deletion (marked with chloramphenicol) strains are described in detail in the Supplemental Experimental Procedures.

#### ACCESSION NUMBERS

The coordinates for the YchM-ACP complex has been deposited at the RCSB with the PDB ID code 3NY7.

#### SUPPLEMENTAL INFORMATION

Supplemental Information includes Supplemental Experimental Procedures, four figures, and two tables and can be found with this article online at doi:10.1016/j.str.2010.08.015.

#### ACKNOWLEDGMENTS

We thank Charles Rock (St. Jude's Research Hospital, Memphis, TN) for ACP antibody and members of the A.E., J.F.G., R.A.F.R. (Jing Li), N.C.J.S., and T.F.M. laboratories for technical assistance. This work was supported by a Canadian Institutes of Health Research (CIHR) grants (82852) to A.E. and J.F.G., and (FRN15266) to R.A.F.R., as well as with instrumentation and infrastructure support provided by Canadian Foundation for Innovation (CFI), Alberta Heritage Foundation for Medical Research (AHFMR), the Michael Smith Foundation for Health Research (MSFHR), and the CIHR. N.C.J.S. is a MSFHR Senior Scholar, CIHR Investigator, and Howard Hughes Medical Institute International Scholar. This project was initiated during a sabbatical leave by R.A.F.R. in the laboratory of N.C.J.S.

Received: May 6, 2010

Revised: August 23, 2010

Accepted: August 26, 2010

Published: November 9, 2010

#### REFERENCES

- Anderson, M.S., and Raetz, C.R. (1987). Biosynthesis of lipid A precursors in *Escherichia coli*. A cytoplasmic acyltransferase that converts UDP-N-acetylglucosamine to UDP-3-O-(R-3-hydroxymyristoyl)-N-acetylglucosamine. *J. Biol. Chem.* 262, 5159–5169.
- Aravind, L., and Koonin, E.V. (2000). The STAS domain—a link between anion transporters and antisigma-factor antagonists. *Curr. Biol.* 10, R53–R55.
- Baba, T., Ara, T., Hasegawa, M., Takai, Y., Okumura, Y., Baba, M., Datsenko, K.A., Tomita, M., Wanner, B.L., and Mori, H. (2006). Construction of *Escherichia coli* K-12 in-frame, single-gene knockout mutants: the Keio collection. *Mol. Syst. Biol.* 2, 10.1038/msb4100050, 2006.0008.
- Babu, M., Butland, G., Pogoutse, O., Li, J., Greenblatt, J.F., and Emili, A. (2009a). Sequential peptide affinity purification system for the systematic isolation and identification of protein complexes from *Escherichia coli*. *Methods Mol. Biol.* 564, 373–400.
- Babu, M., Musso, G., Diaz-Mejia, J.J., Butland, G., Greenblatt, J.F., and Emili, A. (2009b). Systems-level approaches for identifying and analyzing genetic interaction networks in *Escherichia coli* and extensions to other prokaryotes. *Mol. Biosyst.* 5, 1439–1455.
- Butland, G., Babu, M., Diaz-Mejia, J.J., Bohdana, F., Phanse, S., Gold, B., Yang, W., Li, J., Gagarinova, A.G., Pogoutse, O., et al. (2008). eSGA: *E. coli* synthetic genetic array analysis. *Nat. Methods* 5, 789–795.
- Butland, G., Peregrin-Alvarez, J.M., Li, J., Yang, W., Yang, X., Canadien, V., Starostine, A., Richards, D., Beattie, B., Krogan, N., et al. (2005). Interaction network containing conserved and essential protein complexes in *Escherichia coli*. *Nature* 433, 531–537.

- Byers, D.M., and Gong, H. (2007a). Acyl carrier protein: structure-function relationships in a conserved multifunctional protein family. *Biochem. Cell Biol.* **85**, 649–662.
- Byers, D.M., and Gong, H. (2007b). Acyl carrier protein: structure-function relationships in a conserved multifunctional protein family. *Biochem. Cell Biol.* **85**, 649–662.
- Chang, M.H., Plata, C., Sincic, A., Ranatunga, W.K., Chen, A.P., Zandi-Nejad, K., Chan, K.W., Thompson, J., Mount, D.B., and Romero, M.F. (2009). Slc26a9 is inhibited by the R-region of the cystic fibrosis transmembrane conductance regulator via the STAS domain. *J. Biol. Chem.* **284**, 28306–28318.
- Díaz-Mejía, J.J., Babu, M., and Emili, A. (2009). Computational and experimental approaches to chart the *Escherichia coli* cell-envelope-associated proteome and interactome. *FEMS Microbiol. Rev.* **33**, 66–97.
- Dorwart, M.R., Shcheynikov, N., Baker, J.M., Forman-Kay, J.D., Muallem, S., and Thomas, P.J. (2008a). Congenital chloride-losing diarrhea causing mutations in the STAS domain result in misfolding and mistrafficking of SLC26A3. *J. Biol. Chem.* **283**, 8711–8722.
- Dorwart, M.R., Shcheynikov, N., Yang, D., and Muallem, S. (2008b). The solute carrier 26 family of proteins in epithelial ion transport. *Physiology (Bethesda)* **23**, 104–114.
- Endeward, V., Musa-Aziz, R., Cooper, G.J., Chen, L.M., Pelletier, M.F., Virkki, L.V., Supuran, C.T., King, L.S., Boron, W.F., and Gros, G. (2006). Evidence that aquaporin 1 is a major pathway for CO<sub>2</sub> transport across the human erythrocyte membrane. *FASEB J.* **20**, 1974–1981.
- Everett, L.A., and Green, E.D. (1999). A family of mammalian anion transporters and their involvement in human genetic diseases. *Hum. Mol. Genet.* **8**, 1883–1891.
- Everett, L.A., Glaser, B., Beck, J.C., Idol, J.R., Buchs, A., Heyman, M., Adawi, F., Hazani, E., Nassir, E., Baxevanis, A.D., et al. (1997). Pendred syndrome is caused by mutations in a putative sulphate transporter gene (PDS). *Nat. Genet.* **17**, 411–422.
- Felce, J., and Saier, M.H. (2004). Carbonic anhydrases fused to anion transporters of the SulP family: evidence for a novel type of bicarbonate transporter. *J. Mol. Microbiol. Biotechnol.* **8**, 169–176.
- Feng, Y., and Cronan, J.E. (2009). A new member of the *Escherichia coli* fad regulon: transcriptional regulation of fadM (ybaW). *J. Bacteriol.* **191**, 6320–6328.
- Gillam, M.P., Sidhaye, A.R., Lee, E.J., Rutishauser, J., Stephan, C.W., and Kopp, P. (2004). Functional characterization of pendrin in a polarized cell system. Evidence for pendrin-mediated apical iodide efflux. *J. Biol. Chem.* **279**, 13004–13010.
- Henry, M.F., and Cronan, J.E., Jr. (1991). *Escherichia coli* transcription factor that both activates fatty acid synthesis and represses fatty acid degradation. *J. Mol. Biol.* **222**, 843–849.
- Hillier, A.J., and Jago, G.R. (1978). The metabolism of [14C]bicarbonate by *Streptococcus lactis*: the fixation of [14C]bicarbonate by pyruvate carboxylase. *J. Dairy Res.* **45**, 433–444.
- Homma, K., Miller, K.K., Anderson, C.T., Sengupta, S., Du, G.G., Aguiñaga, S., Cheatham, M., Dallos, P., and Zheng, J. (2010). Interaction between CFTR and prestin (SLC26A5). *Biochim. Biophys. Acta* **1798**, 1029–1040.
- Hu, P., Janga, S.C., Babu, M., Díaz-Mejía, J.J., Butland, G., Yang, W., Pogoutse, O., Guo, X., Phanse, S., Wong, P., et al. (2009). Global functional atlas of *Escherichia coli* encompassing previously uncharacterized proteins. *PLoS Biol.* **7**, e96. 10.1371/journal.pbio.1000096.
- Jiang, Z., Grichtchenko, I.I., Boron, W.F., and Aronson, P.S. (2002). Specificity of anion exchange mediated by mouse Slc26a6. *J. Biol. Chem.* **277**, 33963–33967.
- Kim, K.H., Shcheynikov, N., Wang, Y., and Muallem, S. (2005). SLC26A7 is a Cl<sup>-</sup> channel regulated by intracellular pH. *J. Biol. Chem.* **280**, 6463–6470.
- Ko, S.B., Shcheynikov, N., Choi, J.Y., Luo, X., Ishibashi, K., Thomas, P.J., Kim, J.Y., Kim, K.H., Lee, M.G., Naruse, S., and Muallem, S. (2002). A molecular mechanism for aberrant CFTR-dependent HCO<sub>3</sub><sup>-</sup> transport in cystic fibrosis. *EMBO J.* **21**, 5662–5672.
- Kovacs, H., Comfort, D., Lord, M., Campbell, I.D., and Yudkin, M.D. (1998). Solution structure of SpoIIAA, a phosphorylatable component of the system that regulates transcription factor sigmaF of *Bacillus subtilis*. *Proc. Natl. Acad. Sci. USA* **95**, 5067–5071.
- Kozliak, E.I., Fuchs, J.A., Guilloton, M.B., and Anderson, P.M. (1995). Role of bicarbonate/CO<sub>2</sub> in the inhibition of *Escherichia coli* growth by cyanate. *J. Bacteriol.* **177**, 3213–3219.
- Magnuson, K., Jackowski, S., Rock, C.O., and Cronan, J.E., Jr. (1993). Regulation of fatty acid biosynthesis in *Escherichia coli*. *Microbiol. Rev.* **57**, 522–542.
- Mäkelä, S., Kere, J., Holmberg, C., and Höglund, P. (2002). SLC26A3 mutations in congenital chloride diarrhea. *Hum. Mutat.* **20**, 425–438.
- Melvin, J.E., Park, K., Richardson, L., Schultheis, P.J., and Shull, G.E. (1999). Mouse down-regulated in adenoma (DRA) is an intestinal Cl<sup>-</sup>/HCO<sub>3</sub><sup>-</sup> exchanger and is up-regulated in colon of mice lacking the NHE3 Na<sup>+</sup>/H<sup>+</sup> exchanger. *J. Biol. Chem.* **274**, 22855–22861.
- Merlin, C., Masters, M., McAteer, S., and Coulson, A. (2003). Why is carbonic anhydrase essential to *Escherichia coli*? *J. Bacteriol.* **185**, 6415–6424.
- Mittag, T., Kay, L., and Forman-Kay, J. (2010). Protein dynamics and conformational disorder in molecular recognition. *J. Mol. Recognit.* **23**, 105–116.
- Mount, D.B., and Romero, M.F. (2004). The SLC26 gene family of multifunctional anion exchangers. *Pflugers Arch.* **447**, 710–721.
- Musa-Aziz, R., Chen, L.M., Pelletier, M.F., and Boron, W.F. (2009). Relative CO<sub>2</sub>/NH<sub>3</sub> selectivities of AQP1, AQP4, AQP5, AmtB, and RhAG. *Proc. Natl. Acad. Sci. USA* **106**, 5406–5411.
- Nie, L., Ren, Y., Janakiraman, A., Smith, S., and Schulz, H. (2008). A novel paradigm of fatty acid beta-oxidation exemplified by the thioesterase-dependent partial degradation of conjugated linoleic acid that fully supports growth of *Escherichia coli*. *Biochemistry* **47**, 9618–9626.
- Niki, H., Imamura, R., Kitaoka, M., Yamanaka, K., Ogura, T., and Hiraga, S. (1992). *E. coli* MukB protein involved in chromosome partition forms a homodimer with a rod-and-hinge structure having DNA binding and ATP/GTP binding activities. *EMBO J.* **11**, 5101–5109.
- Pasqualetto, E., Aiello, R., Gesiot, L., Bonetto, G., Bellanda, M., and Battistutta, R. (2010). Structure of the cytosolic portion of the motor protein prestin and functional role of the STAS domain in SLC26/SulP anion transporters. *J. Mol. Biol.* **400**, 448–462.
- Prasad, G.V., Coury, L.A., Finn, F., and Zeidel, M.L. (1998). Reconstituted aquaporin 1 water channels transport CO<sub>2</sub> across membranes. *J. Biol. Chem.* **273**, 33123–33126.
- Price, G.D., Woodger, F.J., Badger, M.R., Howitt, S.M., and Tucker, L. (2004). Identification of a SulP-type bicarbonate transporter in marine cyanobacteria. *Proc. Natl. Acad. Sci. USA* **101**, 18228–18233.
- Reithmeier, R.A. (2001). A membrane metabolon linking carbonic anhydrase with chloride/bicarbonate anion exchangers. *Blood Cells Mol. Dis.* **27**, 85–89.
- Rock, C.O., and Jackowski, S. (1982). Regulation of phospholipid synthesis in *Escherichia coli*. Composition of the acyl-acyl carrier protein pool in vivo. *J. Biol. Chem.* **257**, 10759–10765.
- Roujeinikova, A., Simon, W.J., Gilroy, J., Rice, D.W., Rafferty, J.B., and Slabas, A.R. (2007). Structural studies of fatty acyl-(acyl carrier protein) thioesters reveal a hydrophobic binding cavity that can expand to fit longer substrates. *J. Mol. Biol.* **365**, 135–145.
- Shcheynikov, N., Yang, D., Wang, Y., Zeng, W., Karniski, L.P., So, I., Wall, S.M., and Muallem, S. (2008). The Slc26a4 transporter functions as an electroneutral Cl<sup>-</sup>/HCO<sub>3</sub><sup>-</sup> exchanger: role of Slc26a4 and Slc26a6 in I<sup>-</sup> and HCO<sub>3</sub><sup>-</sup> secretion and in regulation of CFTR in the parotid duct. *J. Physiol.* **586**, 3813–3824.
- Shelden, M.C., Howitt, S.M., and Price, G.D. (2010). Membrane topology of the cyanobacterial bicarbonate transporter, BicA, a member of the SulP (SLC26A) family. *Mol. Membr. Biol.* **27**, 12–23.
- Shibagaki, N., and Grossman, A.R. (2004). Probing the function of STAS domains of the Arabidopsis sulfate transporters. *J. Biol. Chem.* **279**, 30791–30799.

- Wakil, S.J., Titchener, E.B., and Gibson, D.M. (1958a). Evidence for the participation of biotin in the enzymic synthesis of fatty acids. *Biochim. Biophys. Acta* 29, 225–226.
- Wakil, S.J., Titchener, E.B., and Gibson, D.M. (1958b). Evidence for the participation of biotin in the enzymic synthesis of fatty acids. *Biochim. Biophys. Acta* 29, 225–226.
- Wu, H.C., Lin, J.J., Chattopadhyay, P.K., and Kanazawa, H. (1980). Biosynthesis and assembly of murein lipoprotein in *Escherichia coli*. *Ann. N Y Acad. Sci.* 343, 368–383.
- Wu, B.N., Zhang, Y.M., Rock, C.O., and Zheng, J.J. (2009). Structural modification of acyl carrier protein by butyryl group. *Protein Sci.* 18, 240–246.
- Xie, Q., Welch, R., Mercado, A., Romero, M.F., and Mount, D.B. (2002). Molecular characterization of the murine Slc26a6 anion exchanger: functional comparison with Slc26a1. *Am. J. Physiol. Renal Physiol.* 283, F826–F838.
- Zolotarev, A.S., Unnikrishnan, M., Shmukler, B.E., Clark, J.S., Vandorpe, D.H., Grigorieff, N., Rubin, E.J., and Alper, S.L. (2008). Increased sulfate uptake by *E. coli* overexpressing the SLC26-related SulP protein Rv1739c from *Mycobacterium tuberculosis*. *Comp. Biochem. Physiol. A Mol. Integr. Physiol.* 149, 255–266.